Experiments with radioactive beams

Thomas Aumann

TECHNISCHE UNIVERSITÄT DARMSTADT
HIC for FAIR — Helmholtz International Center
GSI

May 24th 2016
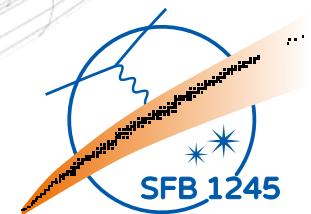
Neutron Skins of Nuclei

mtp: Mainz Institute for Theoretical Physics

SFB 1245

Reactions with neutron-proton asymmetric nuclei

R³B

Reactions with
Relativistic
Radioactive
Beams
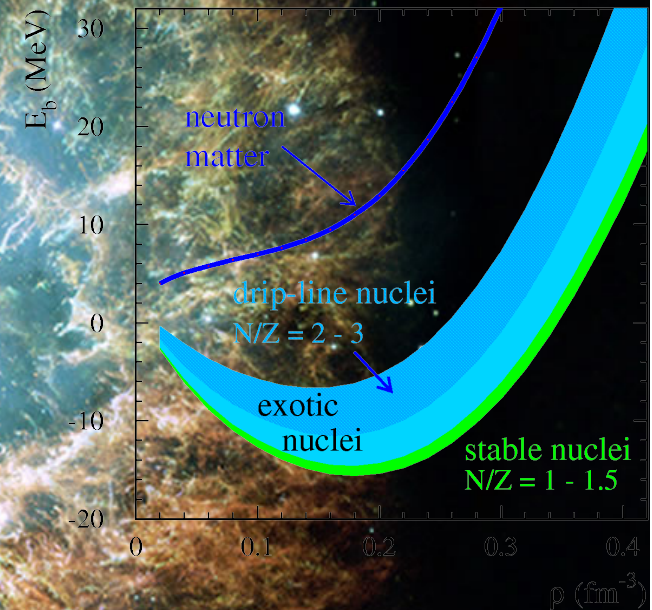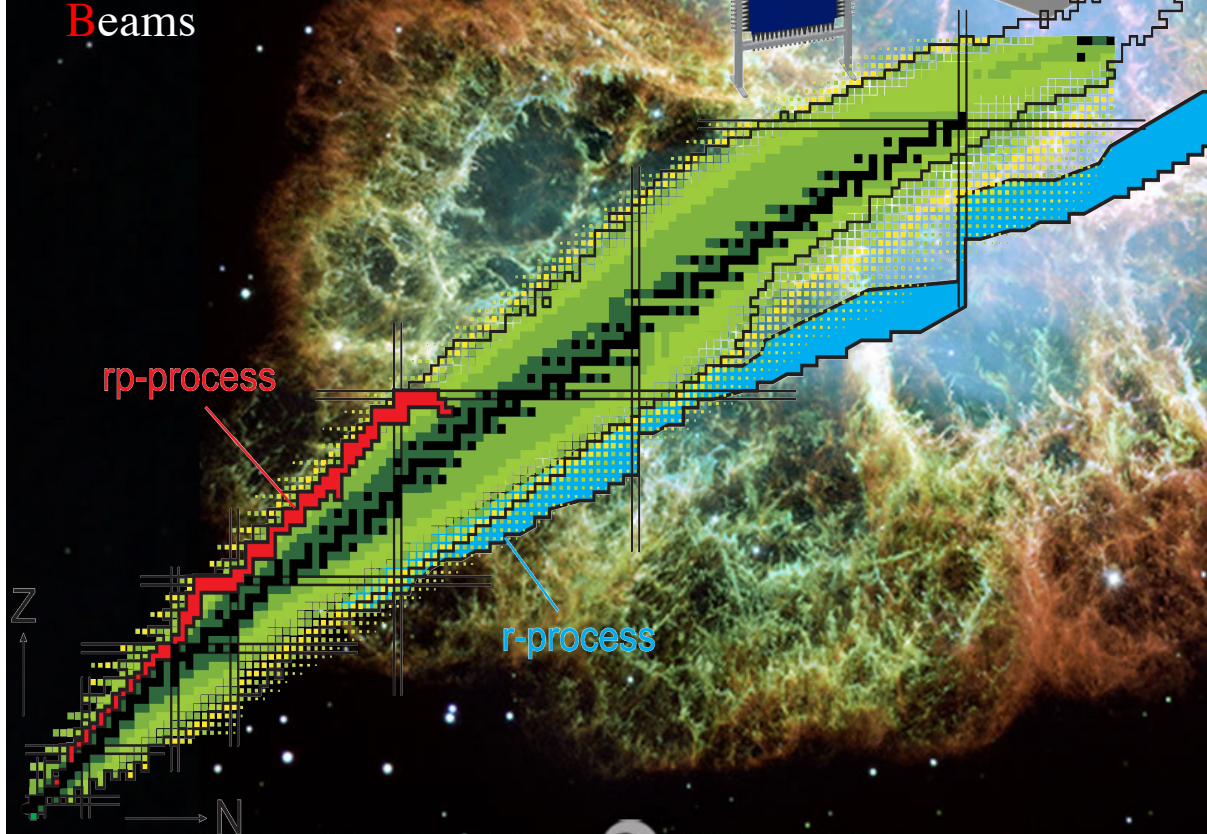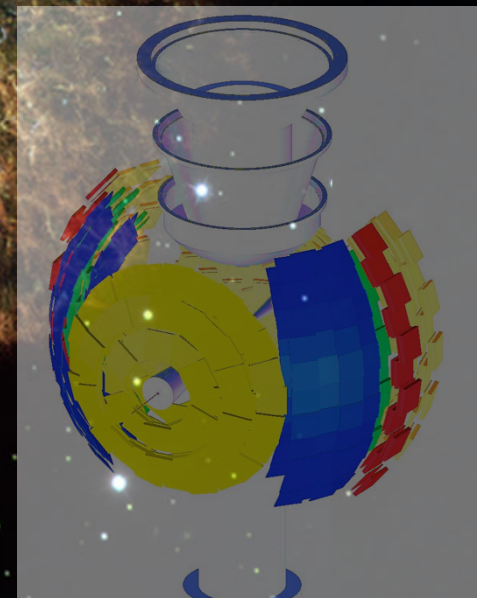
rp-process

r-process

neutron matter

drip-line nuclei
N/Z = 2 - 3

exotic nuclei

stable nuclei
N/Z = 1 - 1.5

E_b (MeV)

ρ (fm^{-3})

Z

N

Reactions with neutron-proton asymmetric nuclei

Reactions with neutron-proton asymmetric nuclei

A laboratory for studying nuclear properties as a function of isospin and density:

Nuclear Structure of exotic nuclei

Neutron-Proton asymmetric matter

Nuclear Astrophysics

rp-process

r-process

Z

N

E_b (MeV)

30

20

10

0

-10

-20

neutron matter

drip-line nuclei
N/Z = 2 - 3

exotic nuclei

stable nuclei
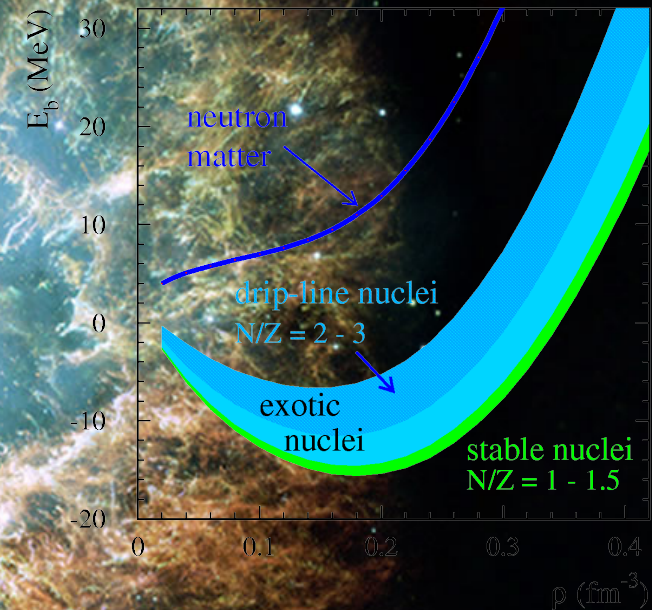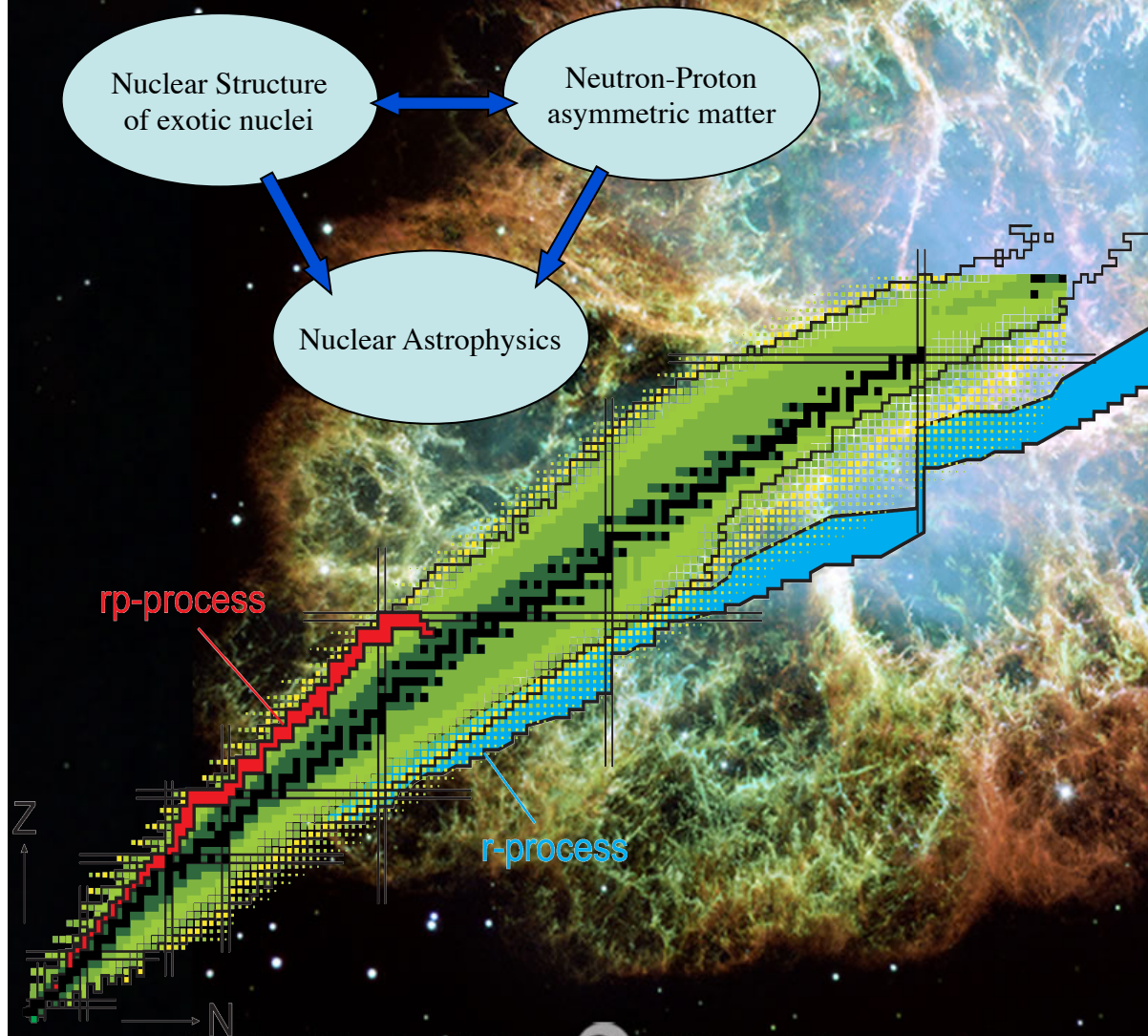N/Z = 1 - 1.5

0   0.1   0.2   0.3   0.4

ρ (fm^{-3})

Reactions with neutron-proton asymmetric nuclei

A laboratory for studying nuclear properties as a function of isospin and density:
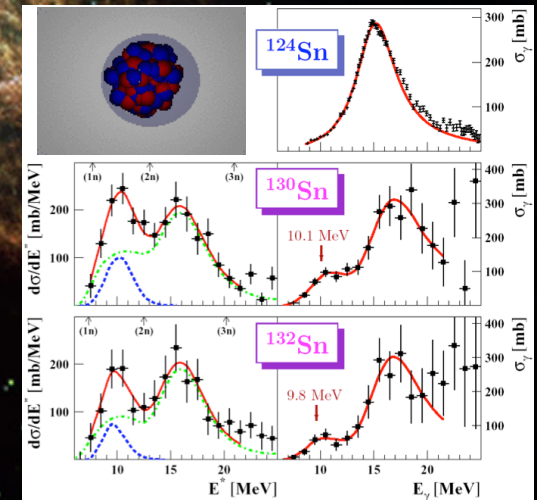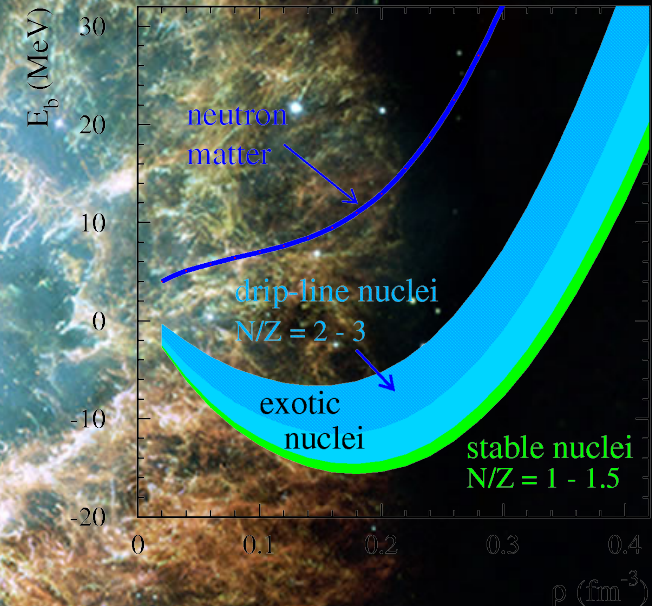
Nuclear Structure of exotic nuclei

Neutron-Proton asymmetric matter

Nuclear Astrophysics

E_b (MeV)

neutron matter

drip-line nuclei
N/Z = 2 - 3

exotic nuclei

stable nuclei
N/Z = 1 - 1.5
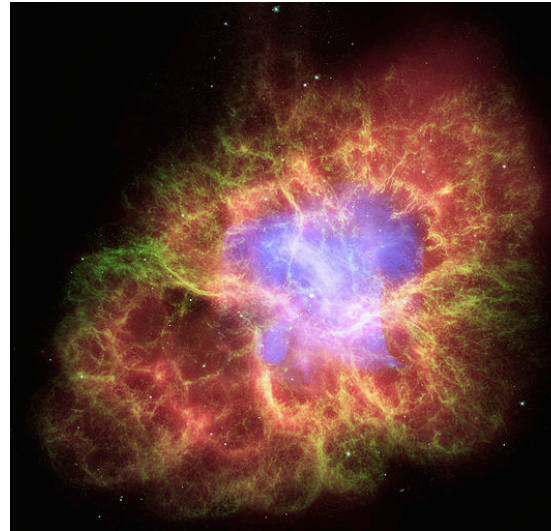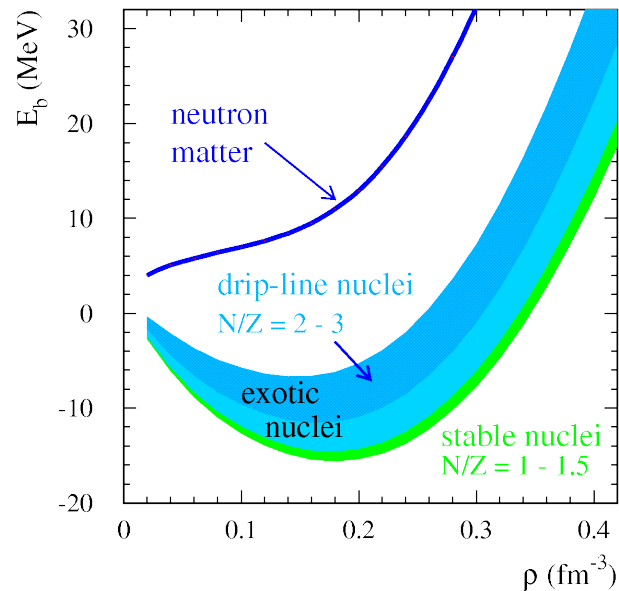
ρ (fm^{-3})

rp-process

r-process

Dipole response of N-Z asymmetric nuclei

- Redistribution of collective strength (Pygmy and Giant Resonances)
- Nucleosynthesis processes
- Symmetry energy (neutron pressure)

^{124}Sn

^{130}Sn
10.1 MeV

^{132}Sn
9.8 MeV

σ_γ [mb]

$d\sigma/dE^*$ [mb/MeV]

$d\sigma/dE^*$ [mb/MeV]

(1n) (2n) (3n)

E* [MeV]

E$_\gamma$ [MeV]
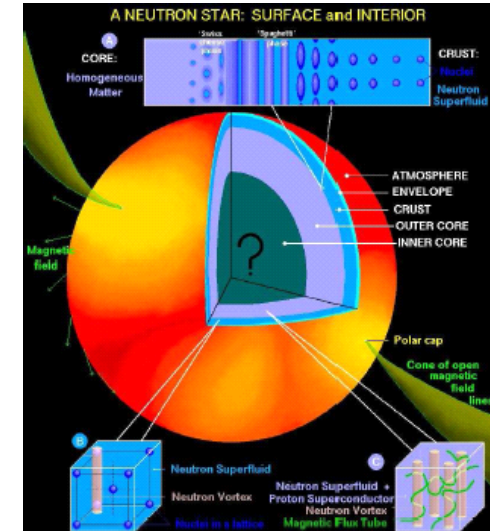
Supernova explosion   Neutron Star

The nuclear equation of state:

dependence on n-p asymmetry and density

symmetry energy at higher densities

$\rightarrow$ reactions with n-rich nuclei ?

symmetry energy and its density dependence close to saturation density

$\rightarrow$ properties of n-rich nuclei ?

<u>Properties of neutron-rich nuclei related to neutron matter</u>

Symmetry energy and slope:

- **Neutron-skin thickness**
- **Dipole response: GDR centroid, Pygmy resonance -> dipole polarizability**
- Quadrupole response: centroid of isovector GQR
- **GMR**
- …

Correlations:
- 3N force -> nuclear structure
- 3neutron force -> structure of n-rich nuclei (at and beyond drip),
  neutron systems (e.g. 4n)
- N-N tensor and short-range correlations -> quasi-free scattering (p,pn); (p,2p)
- Clustering -> quasi-free scattering (p,pα)

Relativistic Coulomb excitation and invariant-mass spectroscopy:
 R3B at GSI and FAIR, EXL at HESR up to 5 GeV/nucleon
-> **Dipole polarizabilty**

Inelastic alpha scattering
 EXL at ESR and/or at HESR at FAIR
-> **Giant Monopole Resonance**

Elastic proton scattering
 EXL at at ESR and/or at HESR at FAIR, active target at R3B
Elastic electron scattering
 SCRIT at RIKEN, ELISe at ESR at FAIR
Isotope shift measurements (LASPEC at FAIR)
-> **Neutron-skin thickness**

? Relativistic Coulomb excitation and missing-mass spectroscopy
 p,p'; a,a'; $^{16}O,^{16}O$ at the storage ring (EXL at ESR and/or HESR)

Total reaction and charge-changing cross sections (see talk of Ritu)
 R3B at GSI and FAIR

Isoscalar giant resonances in the Sn nuclei and implications for the asymmetry term in the nuclear-matter incompressibility
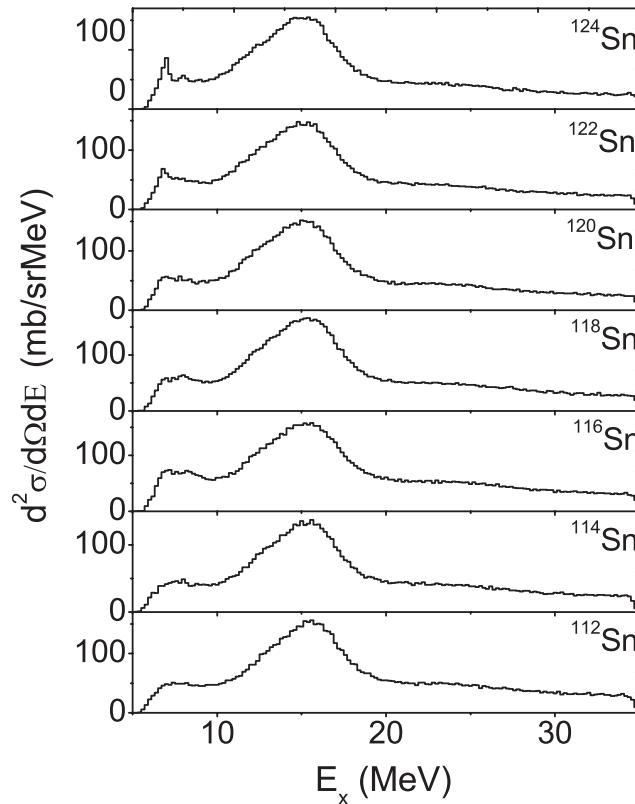
Measurement at RCNP

U. Garg et al.

FIG. 3. Excitation-energy spectra obtained from inelastic α scattering at $\theta_{\mathrm{lab}} = 0.69°$ for all even-A Sn isotopes.
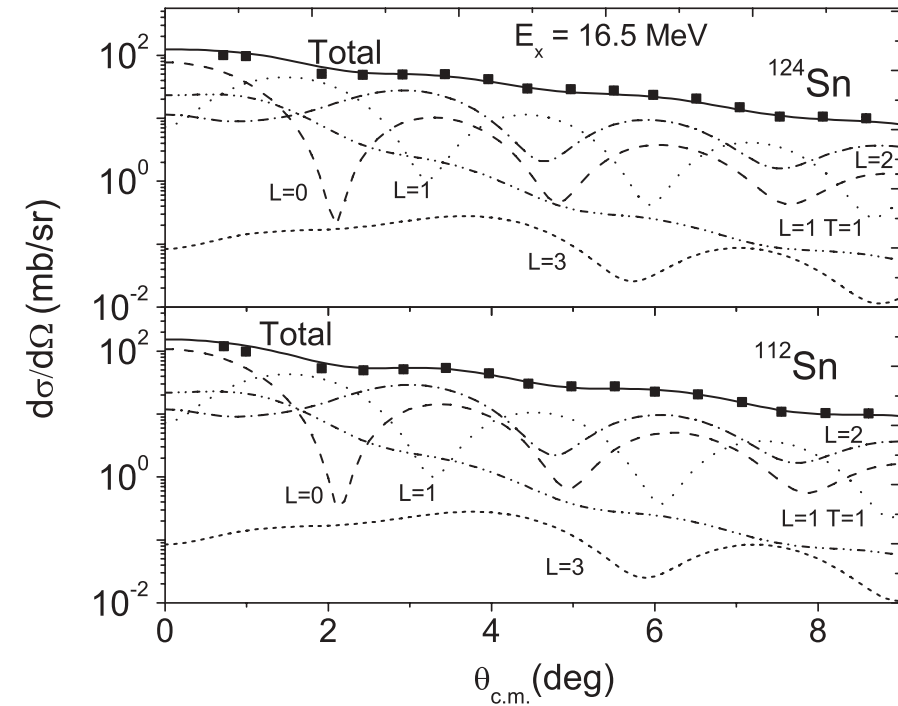

FIG. 7. Angular distribution of 1-MeV bins centered at $E_x = 16.5$ MeV for ^{112}Sn(α, α') and ^{124}Sn(α, α'). The solid squares are the experimental data and the solid lines are the MDA fits to the data. Also shown are the contributions to the fits from $L = 0$ (dashed line), $L = 1$ (dotted line), $L = 2$ (dash-dotted line), and $L = 3$ (small-dashed line) multipoles, as well as from the IVGDR (dash-dot-dotted line).

Low-momentum transfer region often most important, e.g.,

- giant monopole excitation

- elastic scattering

Experimental difficulty

- low recoil energies
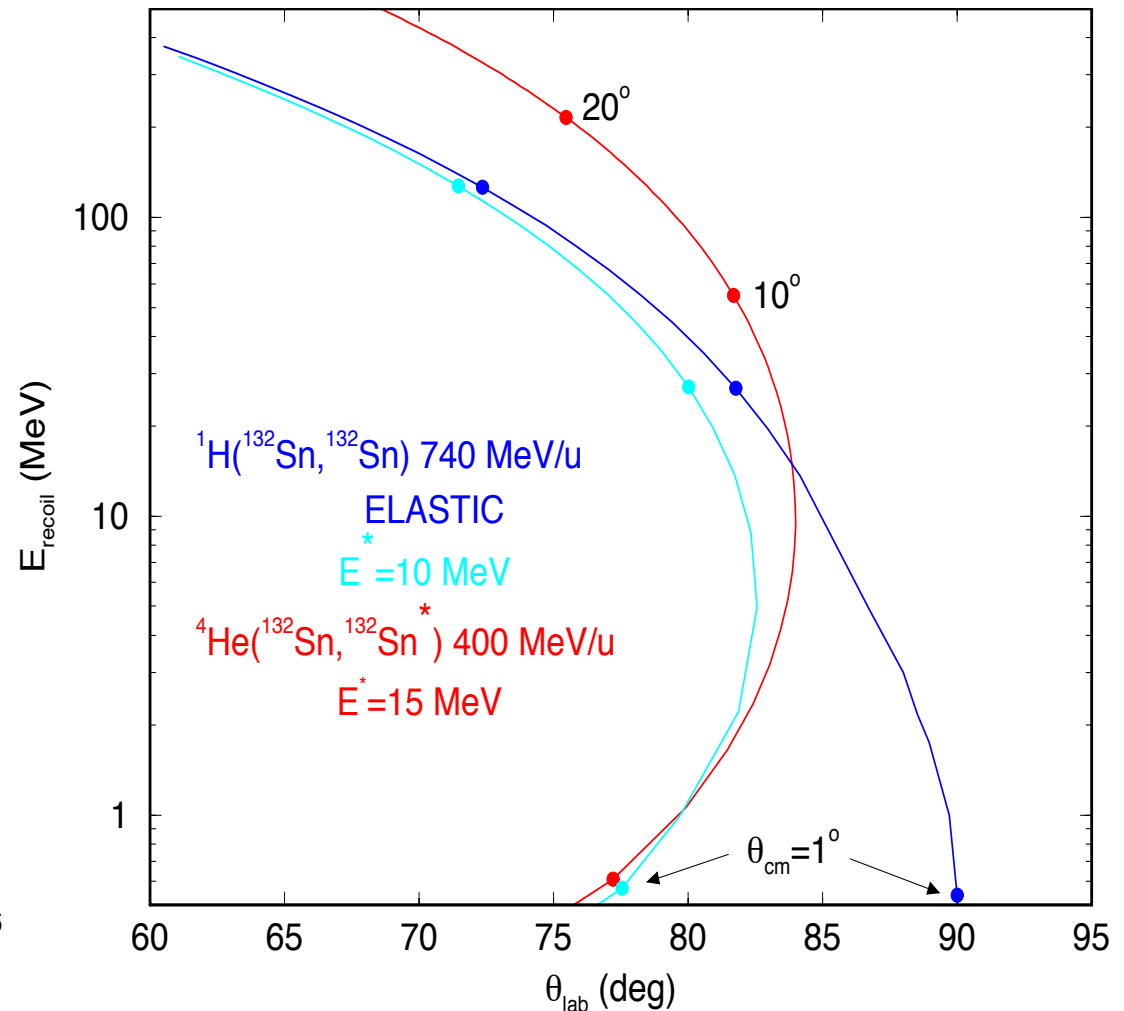
-> thin targets (low luminosity)

Experimental approaches:

- active target

- in-ring scattering at internal gas-jet targets

gaining back luminosity due to circulation frequency of ~ 10^6

$^1H(^{132}Sn, ^{132}Sn)$ 740 MeV/u ELASTIC
$E^* = 10$ MeV

$^4He(^{132}Sn, ^{132}Sn^*)$ 400 MeV/u
$E^* = 15$ MeV

20°

10°

$\theta_{cm} = 1^o$

E_{recoil} (MeV)

θ_{lab} (deg)

Facility for Anti-Proton and Ion Research FAIR

Facility for Anti-Proton and Ion Research FAIR

Primary Beams SIS 100

- 4.5×10^{11} U^{28+} ions/spill; 1.5 GeV/u
- 10^{10}/s $^{238}U^{92+}$ up to 11 GeV/u
- 2×10^{13} protons/spill; 29 GeV

Secondary Beams

- range of radioactive ion beams up to 1.5 - 2 GeV/u; up to a factor of 10'000 higher in intensity than presently
- antiprotons 1.5 - 14.1 GeV

Storage and Cooler Rings

- radioactive ion beams
- antiproton beams:
  CR: 10^8 antiprotons; 3 GeV
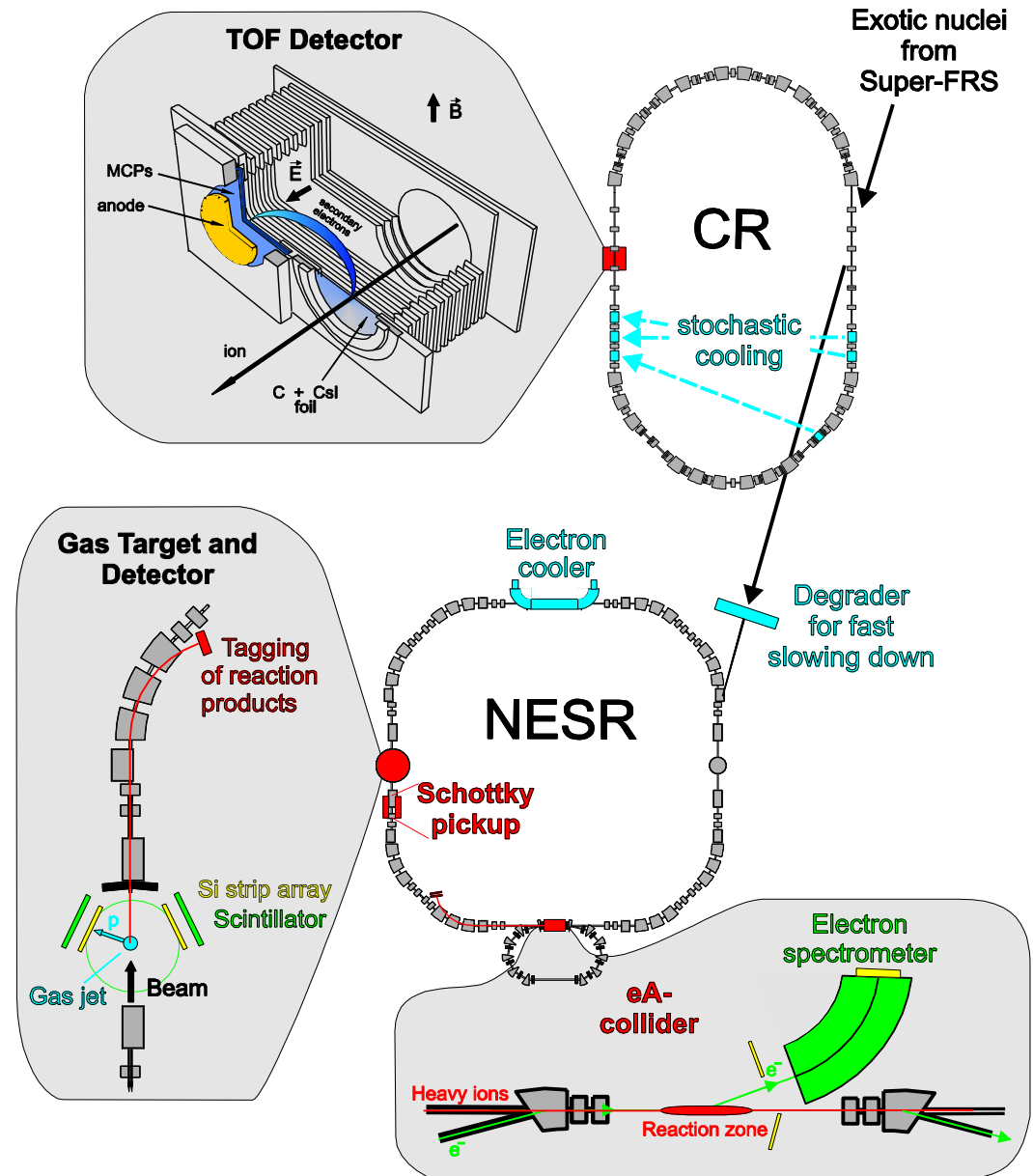 HESR: 10^{10} antiprotons; 1.5 - 14.1 GeV
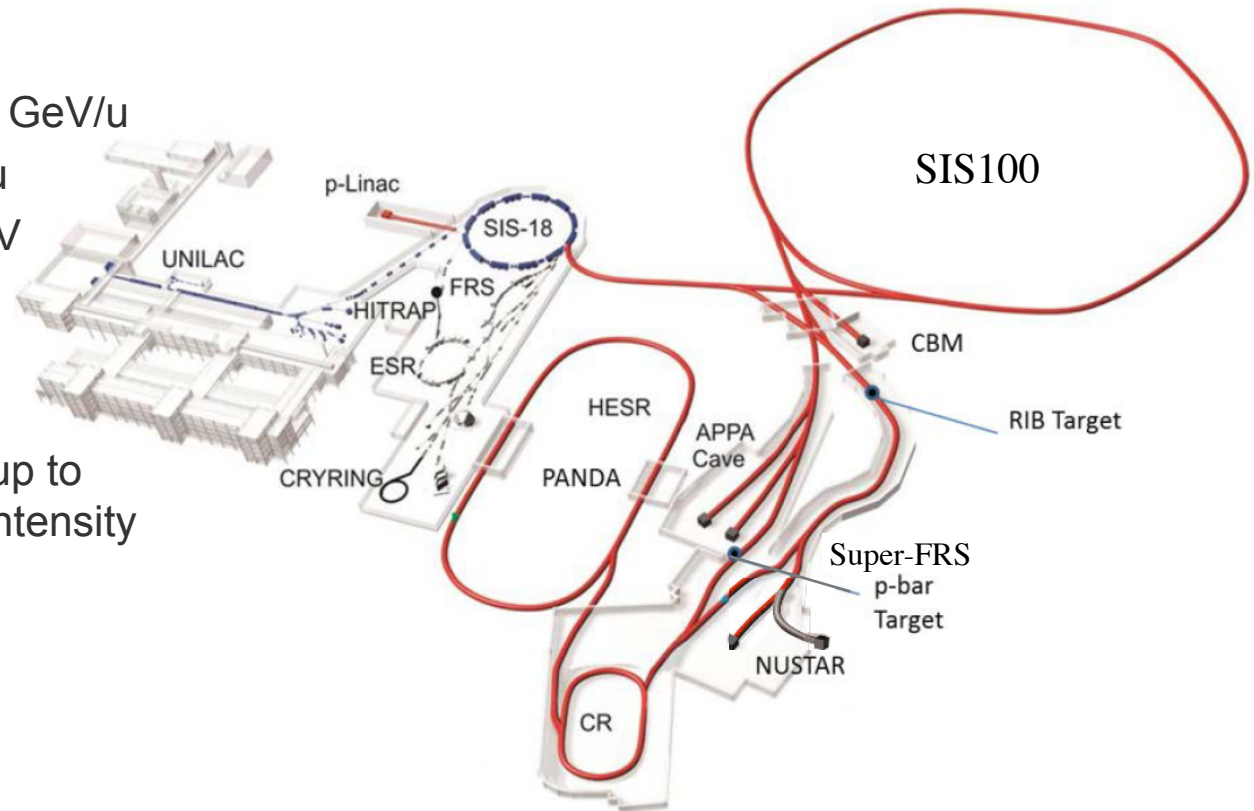
Technical Challenges

- Rapid cycling superconducting magnets
- rf-systems and control
- Beam lifetime (dynamic vacuum)
- Cooled beams

- **Mass measurements**

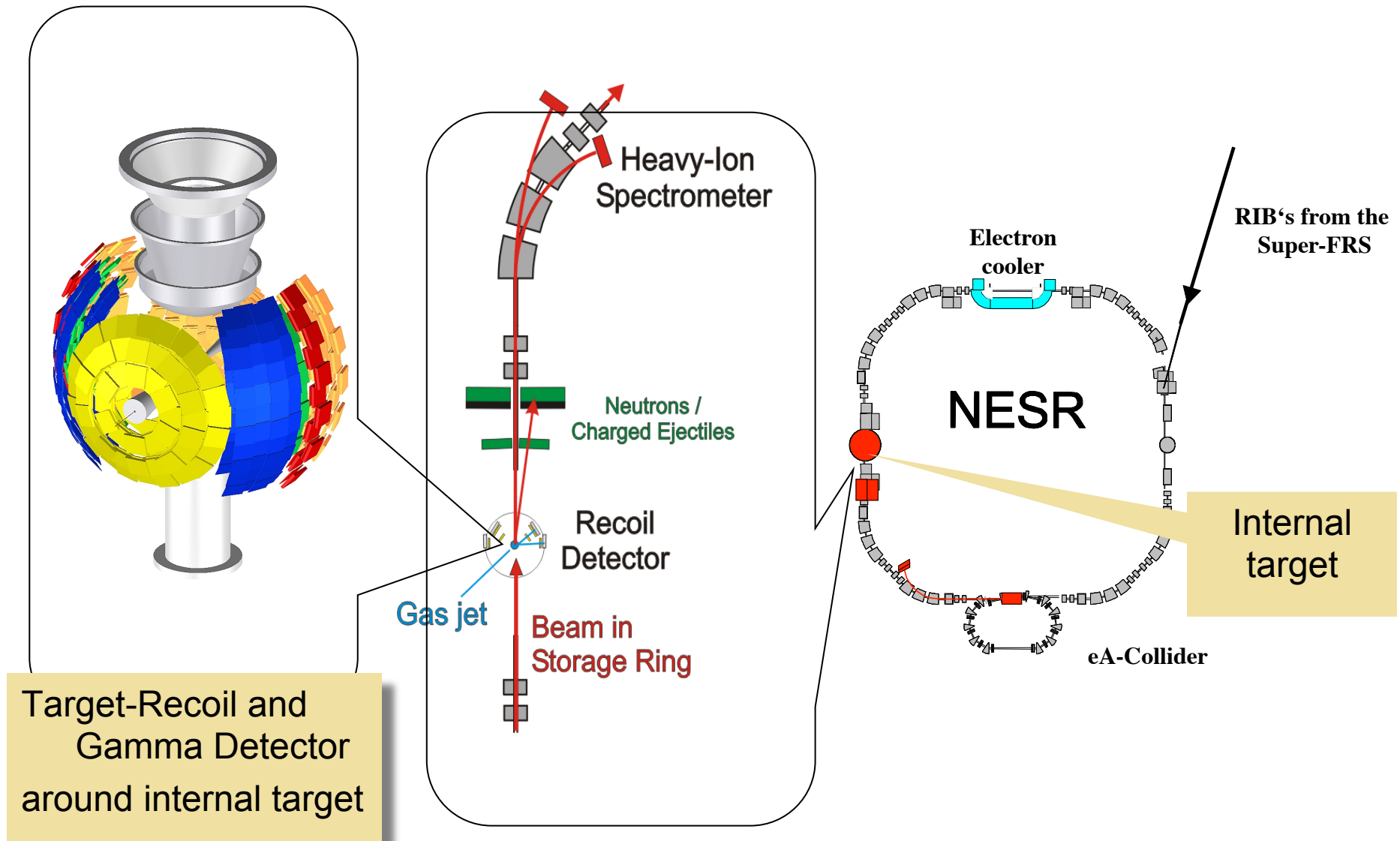- **Reactions with internal targets**
  - Elastic p scatt.
  - (p,p') (α,α')
  - charge-exchange
  - transfer

- **Electron scattering**
  - elastic scattering
  - inelastic

- **Antiproton-A collider**

EXotic Nuclei Studied in **L**ight-Ion Induced Reactions at the NESR Storage Ring

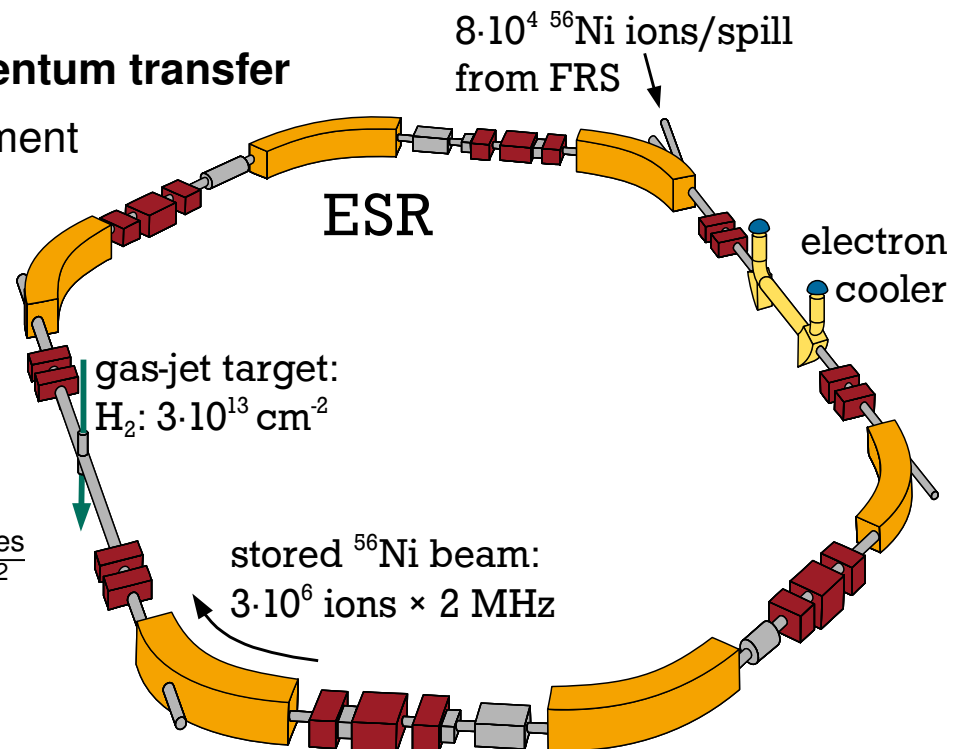Target-Recoil and Gamma Detector around internal target

Heavy-Ion Spectrometer

Neutrons / Charged Ejectiles

Recoil Detector

Gas jet

Beam in Storage Ring

Electron cooler

RIB's from the Super-FRS

NESR

Internal target

eA-Collider

- ▶ "**EX**otic nuclei studied in **L**ight-ion induced reactions at storage rings"

- ▶ **Direct reactions** of exotic beams in **inverse kinematics** on an internal gas-jet target
    - ▶ Measurements at very **low momentum transfer**
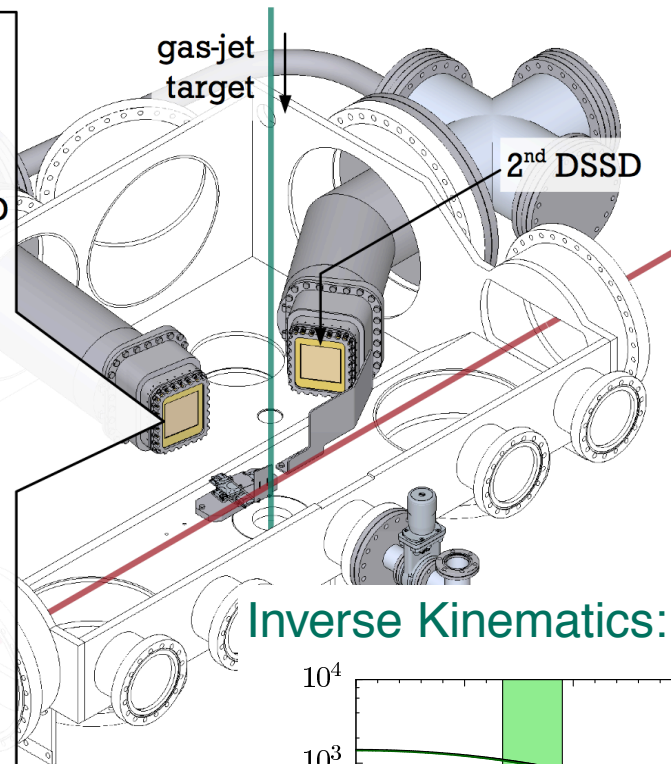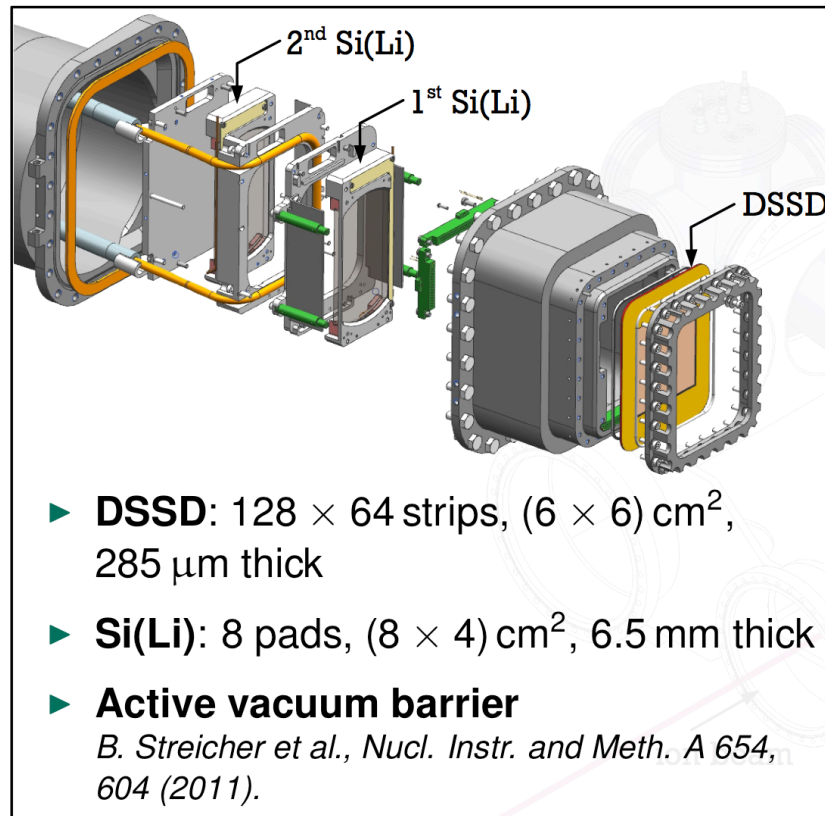   - ▶ Kinematically complete measurement

- ▶ First EXL experiment with radio-active beam at the ESR, GSI:
    - ▶ ^{20}Ne, ^{58}Ni and **^{56}Ni** beams
    - ▶ ^{4}He and **H$_2$** gas-jet targets
    - ▶ ^{56}Ni(p,p) **luminosity**: $2 \cdot 10^{26} \frac{\text{particles}}{\text{s cm}^2}$
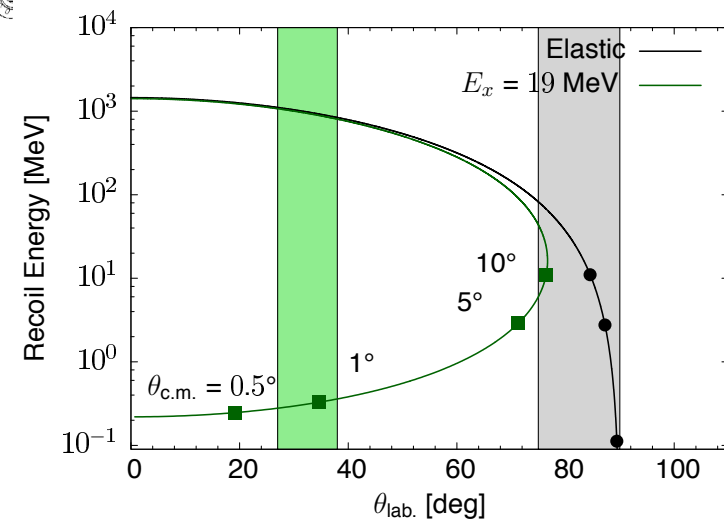

$8 \cdot 10^4$ ^{56}Ni ions/spill from FRS

ESR

electron cooler

gas-jet target: H$_2$: $3 \cdot 10^{13}$ cm^{-2}

stored ^{56}Ni beam: $3 \cdot 10^6$ ions × 2 MHz

Picture: Phys. Scr. T156 (2013) 014016

Mirko von Schmid, TU Darmstadt

- **DSSD**: 128×64 strips, $(6 \times 6)\,\mathrm{cm^2}$, $285\,\mu\mathrm{m}$ thick

- **Si(Li)**: 8 pads, $(8 \times 4)\,\mathrm{cm^2}$, $6.5\,\mathrm{mm}$ thick

- **Active vacuum barrier**
  B. Streicher et al., Nucl. Instr. and Meth. A 654, 604 (2011).

Inverse Kinematics: $\alpha(^{58}\mathrm{Ni}, \alpha')$

Mirko von Schmid, TU Darmstadt
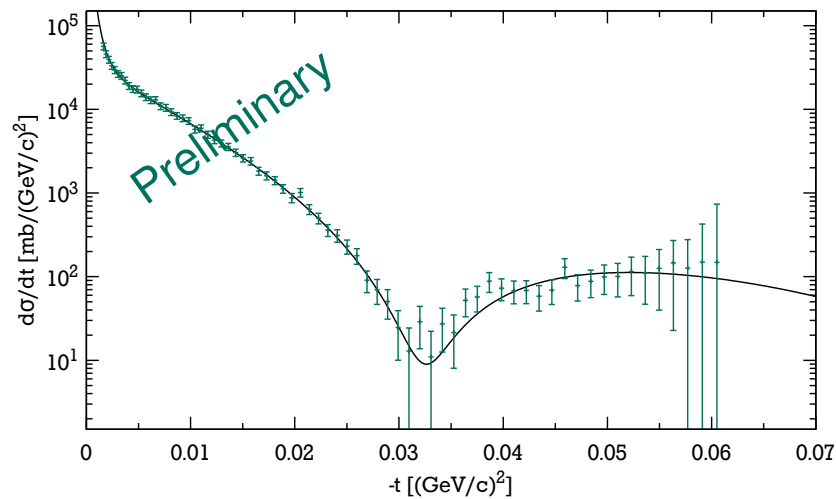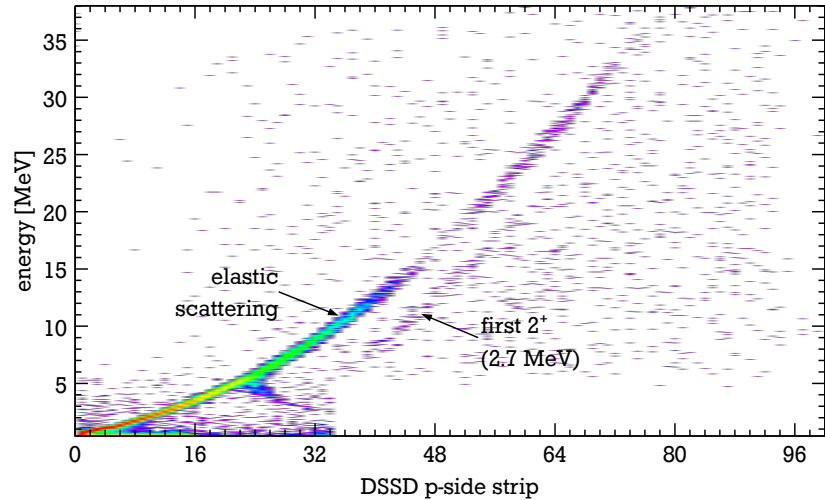
► RMS matter radius: $\langle r_m^2 \rangle^{1/2} = (3.76 \pm 0.08)$ fm
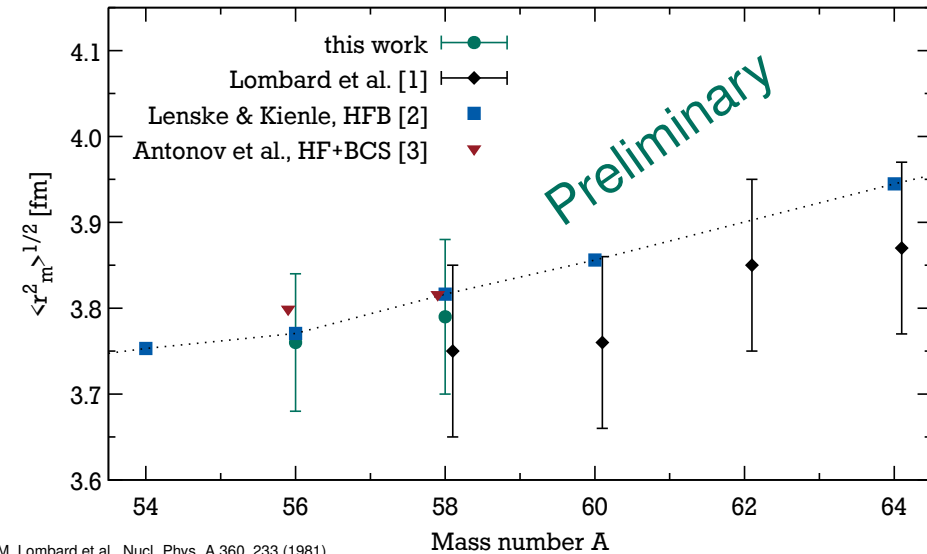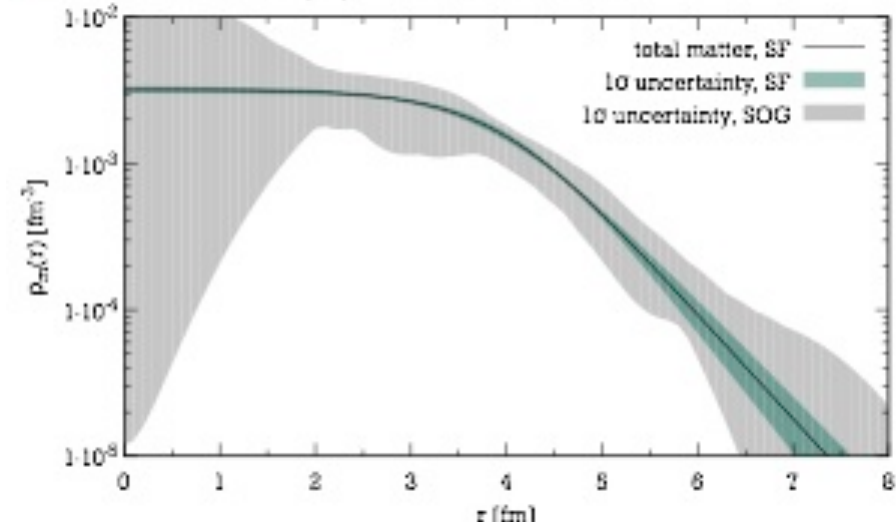
Mirko von Schmid, TU Darmstadt

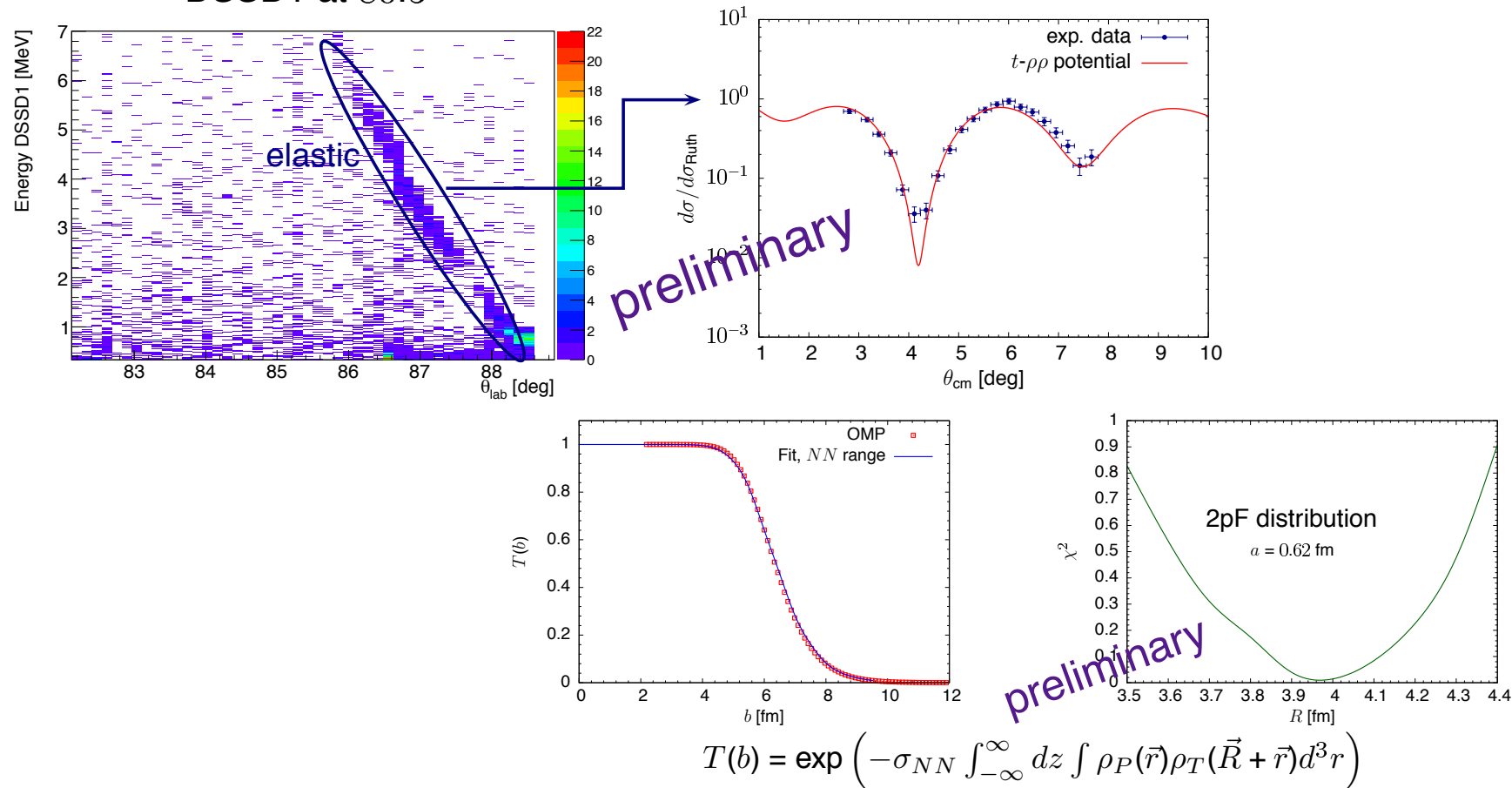[1] R.M. Lombard et al., Nucl. Phys. A 360, 233 (1981)
[2] H. Lenske and P. Kienle, Phys. Lett. B 647, 82 (2007)
[3] A.N. Antonov et al., Phys. Rev. C 72, 044307 (2005)

Elastic alpha scattering off ^{58}Ni (100 MeV/u)

DSSD1 at $80.5°$

$$T(b) = \exp\left(-\sigma_{NN} \int_{-\infty}^{\infty} dz \int \rho_P(\vec{r})\rho_T(\vec{R}+\vec{r})d^3r\right)$$

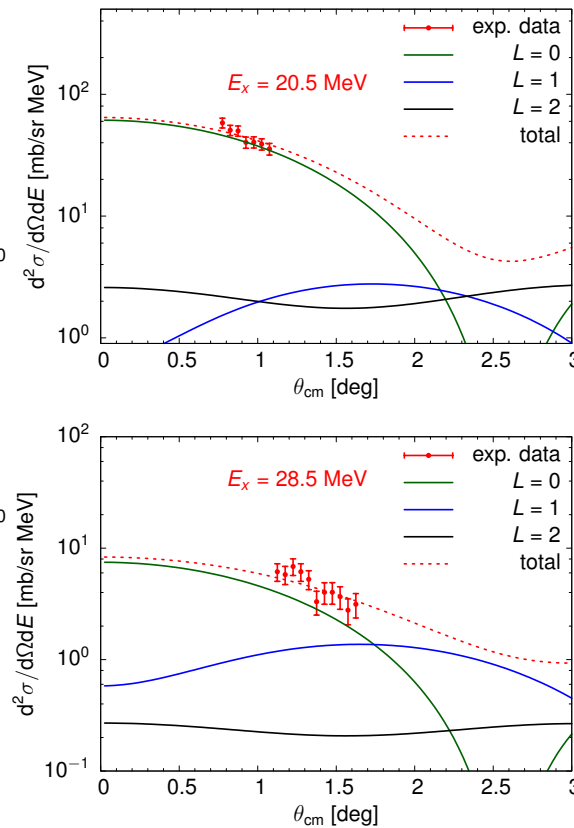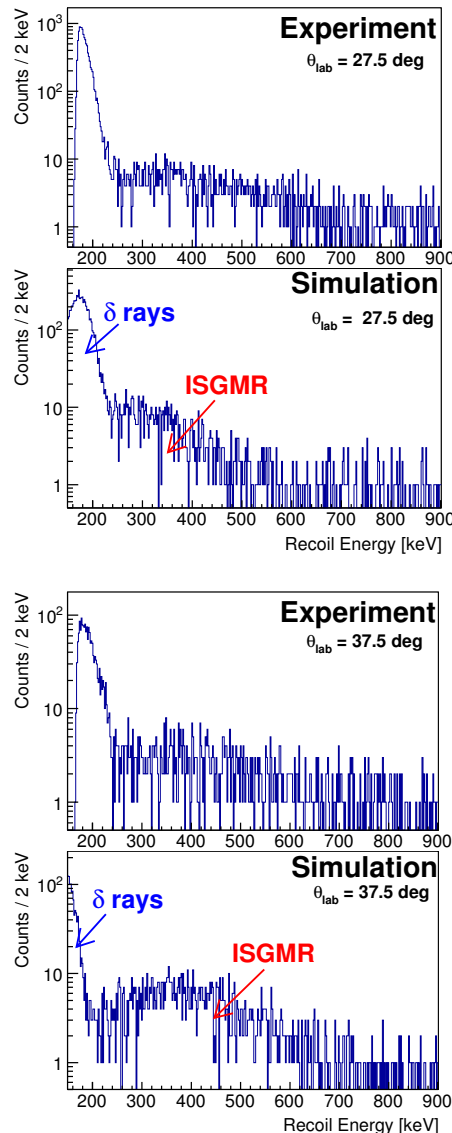$\sqrt{\langle r_m^2 \rangle}$ = 3.71(10) fm: This work
3.66(10) fm: Exp. (α scatt.), Nucl. Phys. A **191**, 145 (1972)
3.65(5) fm: Exp. (p scatt.), Phys. Lett. B **67**, 402 (1977)
3.71 fm: HFB, Phys. Rev. C **72**, 044307 (2005)

Juan Carlos Zamora, TU Darmstadt

Inelastic alpha scattering off ^{58}Ni (100 MeV/u)

Multipole Decomposition Analysis

Preliminary
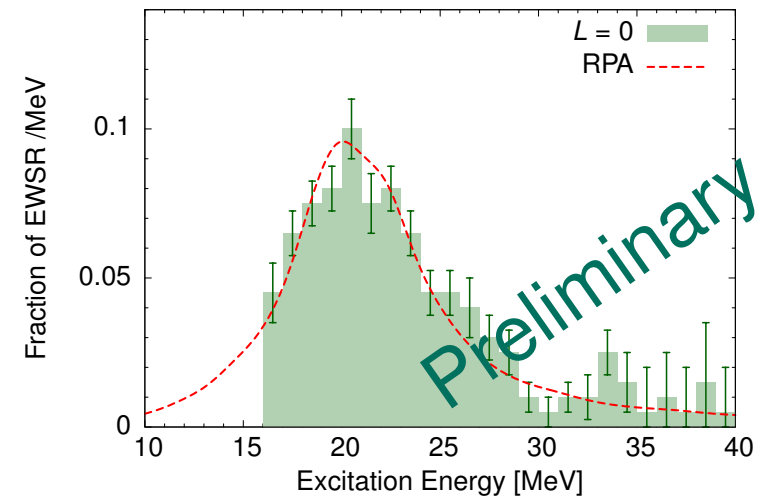
centroid [MeV]	EWSR [%]	
$21.9^{+0.8}_{-1.1}$	79^{+12}_{-11}	present data
$21.5^{+3.0}_{-0.3}$	74^{+22}_{-12}	PRC **61**, 067307 (2000)
$20.8^{+0.9}_{-0.3}$	85^{+13}_{-10}	PRC **73**, 014314 (2006)
21.1	94	RPA calculation [4]

[4] G. Colò et al, Comput. Phys. Commun. 184 (2013)

Giant Monopole Resonance of ^{58}Ni

Juan Carlos Zamora, TU Darmstadt

Symmetry energy and dipole response

polarizability
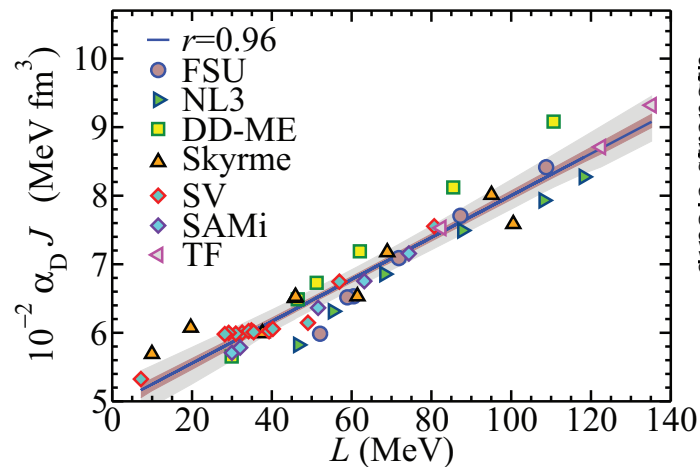dipole response ⟷ density dependence of symmetry energy ⟷ properties of neutron-rich matter

$$\alpha_D = \frac{\hbar c}{2\pi^2} \int_0^\infty \frac{\sigma(E)}{E^2} dE$$

X. Roca-Maza et al., PRC 88 (2013) 024316

neutron skin of ^{208}Pb [fm]
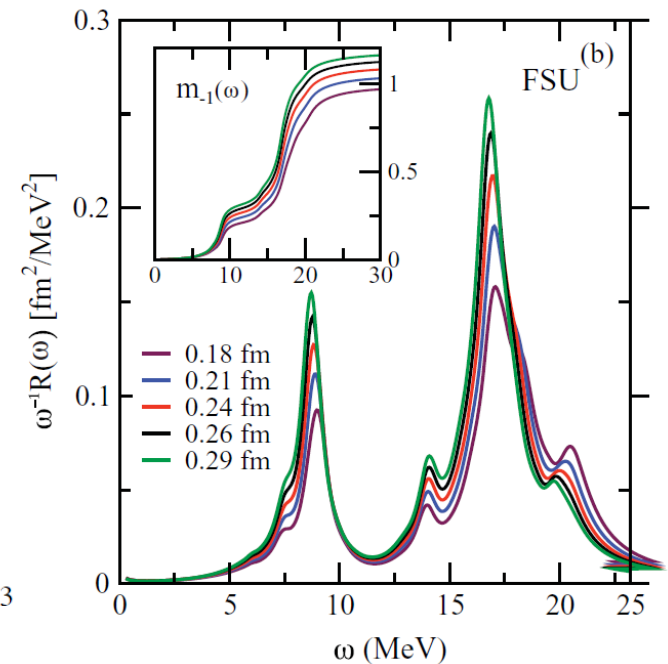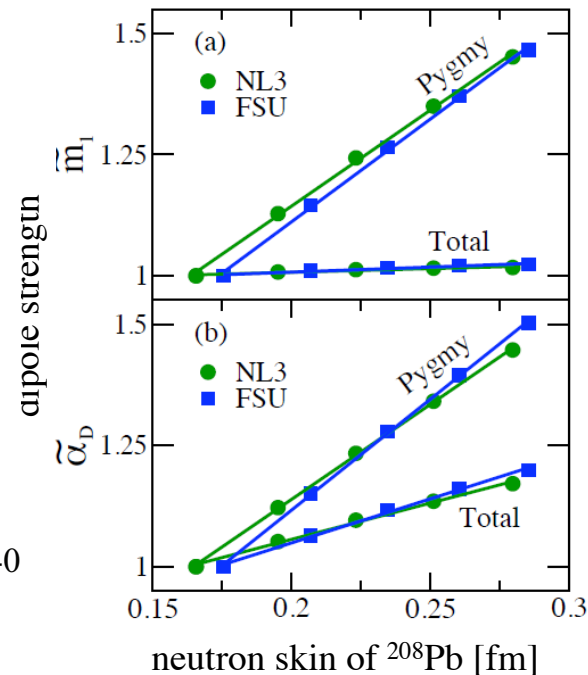
*J. Piekarewicz, PRC **83**, 034319 (2011)*

n-skin / (L, J) from Pygmy strength ⟹

J. Piekarewicz, PRC 73, 044325 (2006)
A. Klimkiewicz et al., PRC 76 (2007) 051603(R)
A. Carbone et al., PRC 81 (2010) 041301(R)

n-skin / (L, J) from polarizability ⟹

P.-G. Reinhard, W. Nazarewicz, PRC 81 (2010) 051303(R)
A. Tamii et al., Phys. Rev. Lett. 107 (2011) 062502.

Relativistic Mean Field Calculation
by Andrea Horvat

Higher sensitivity for n-rich nuclei
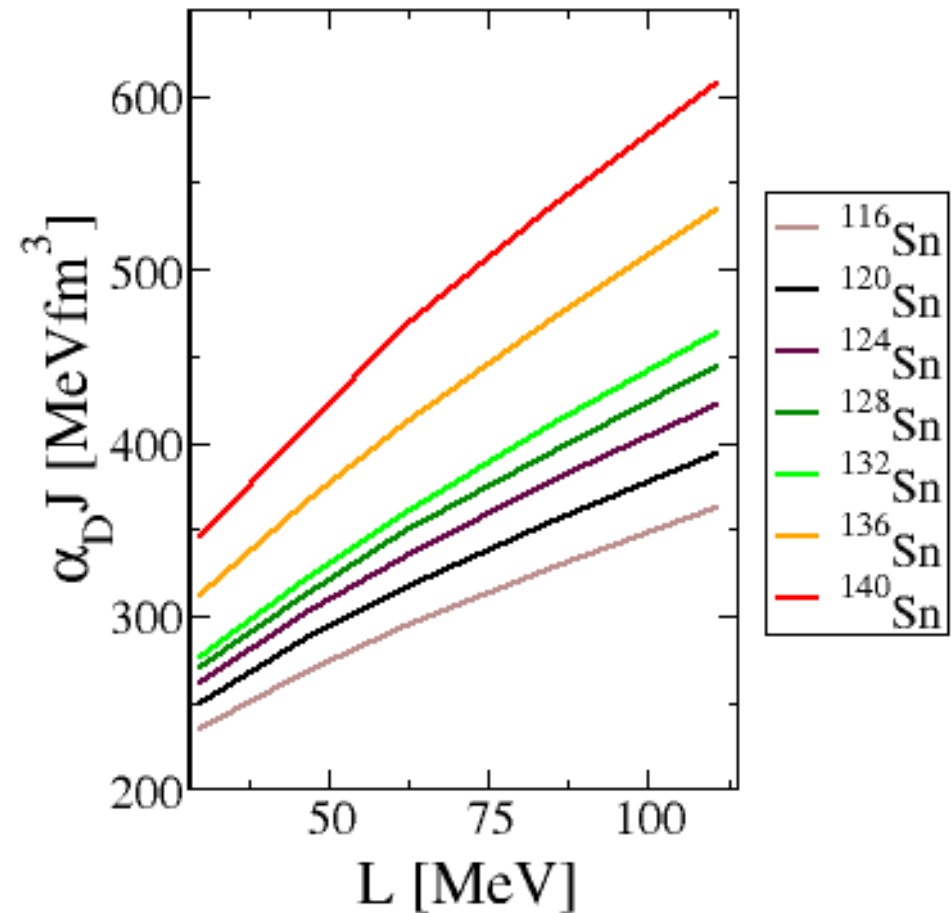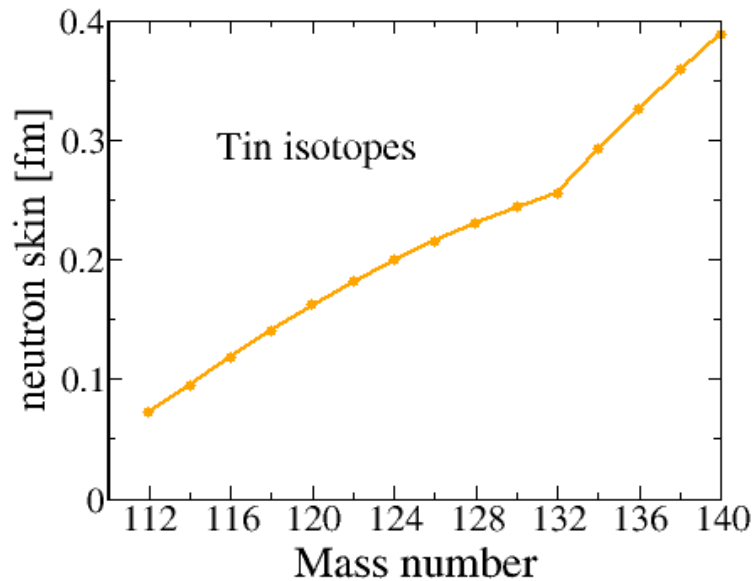
Calculation using RHB+RQRPA framewoork with DD-ME2* effective interaction

*G. A. Lalazissis, T. Nikšić, D. Vretenar, P. Ring, Phys. Rev. C 71 024312 (2005)

$b > R_P + R_T$

Pb

$\sigma_{elm} \sim Z^2$

Absorption of 'virtual Photons'

v~c

A_1, Z_1

b

A_2, Z_2

Semi-classical theory:

$$d\sigma_{elm} / dE = N_\gamma(E) \, \sigma_\gamma(E)$$

σ (mb)

2^+

GDR

10^3

GQR (is)

10^2

2-ph GDR

10

3-ph GDR

1

10^{-1} 1 10

E (GeV/nucleon)
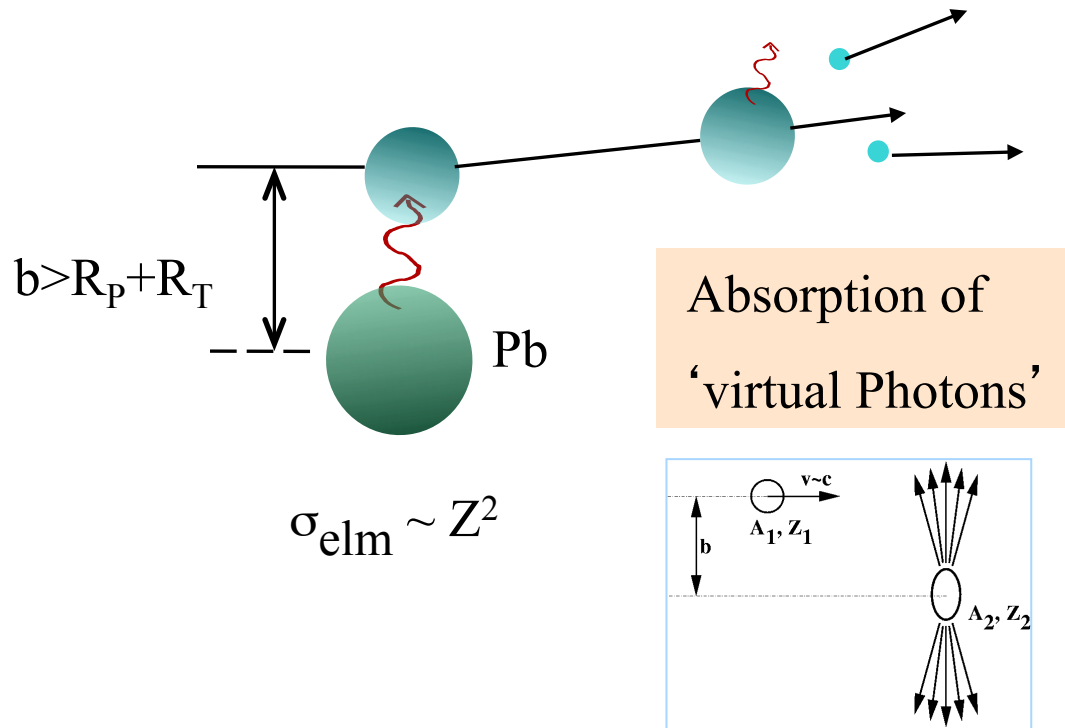
High velocities v/c≈0.6-0.9
⇒ High-frequency Fourier components

$E_{\gamma,max} \approx 25$ MeV (@ 1 GeV/u)
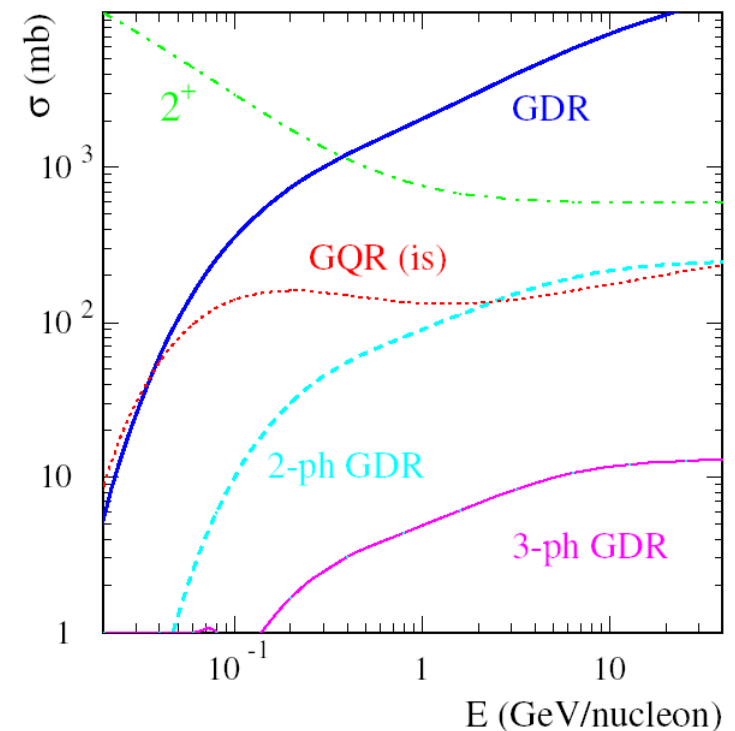
Determination of 'photon energy' (excitation energy) via a kinematically complete measurement of the momenta of all outgoing particles (invariant mass)

- Stable beams from SIS, fragmentation on Be target or in-flight fission
- Selection of radioactive beams in Fragment Separator (FRS)

Bρ − from position at middle focal plane of the FRS

β − from TOF

Z − from ΔE

$$\frac{A}{Z} = \frac{e}{m_u c}\frac{B\rho}{\beta\gamma}$$

Incoming beam identification

^{68}Ni

A/Z

Mixed beam

Charged fragments

ToF, ΔE

tracking → Bρ ~ A/Qβγ

LAND

Neutrons

ToF, x, y, z

~12 m

projectile tracking

Photons

Beam

ALADIN
large-acceptance dipole

Crystal Ball
and Target

Excitation energy E* from kinematically complete measurement of all outgoing particles:

$$E^* = \left(\sqrt{\sum_i m_i^2 + \sum_{i \neq j} m_i m_j \gamma_i \gamma_j (1 - \beta_i \beta_j \cos \theta_{ij})} - m_{proj} \right) c^2 + E_\gamma$$

Mass to charge ratio A/Q

nuclear charge Z

Mixed beam

Charged fragments

ToF, ΔE

tracking $\rightarrow$ Bρ ~ A/Q$\beta\gamma$

LAND

Neutrons

projectile tracking

Photons

~12 m

ALADIN
large-acceptance dipole

GDR

S_{2n}

S_n

PDR

Beam

Crystal Ball
and Target

n

γ_0

n

A-1

γ_0

γ_0

γ'

A

Excitation energy E* from complete measurement of particles:

$$E^* = \left(\sqrt{\sum_i m_i^2 + \sum_{i \neq j} m_i m_j \gamma_i \gamma_j (1 - \beta_i \beta_j \cos \theta_{ij})} - m_{proj} \right) c^2 + E_\gamma$$

Mass to charge ratio A/Q — axis values: 2.56, 2.58, 2.6, 2.62, 2.64, 2.66, 2.68
nuclear charge Z — axis values: 48, 49, 50, 51, 52, 53

Method: Electromagnetic excitation at relativistic beam energies

(C.A. Bertulani and G. Baur, Phys. Rep. 163, 299 (1988))

Electromagnetic-excitation cross section

Photo-neutron cross section

stable

radioactive

^{124}Sn

^{130}Sn

10.1 MeV

^{132}Sn

9.8 MeV

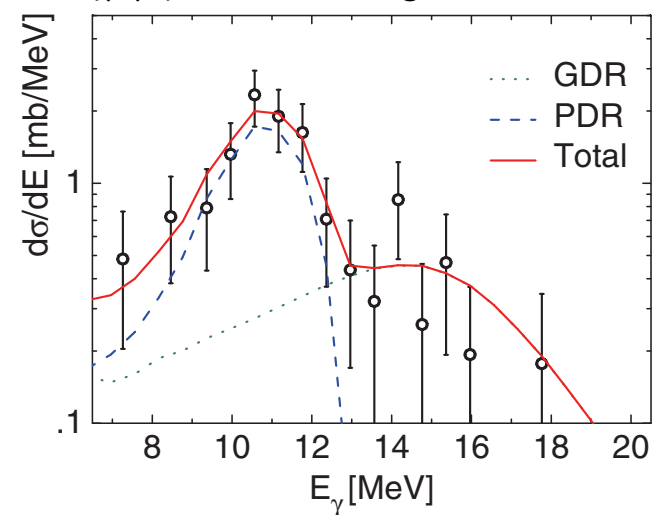(1n) (2n) (3n)

$d\sigma/dE^*$ [mb/MeV]

σ_γ [mb]

E^* [MeV]

E_γ [MeV]
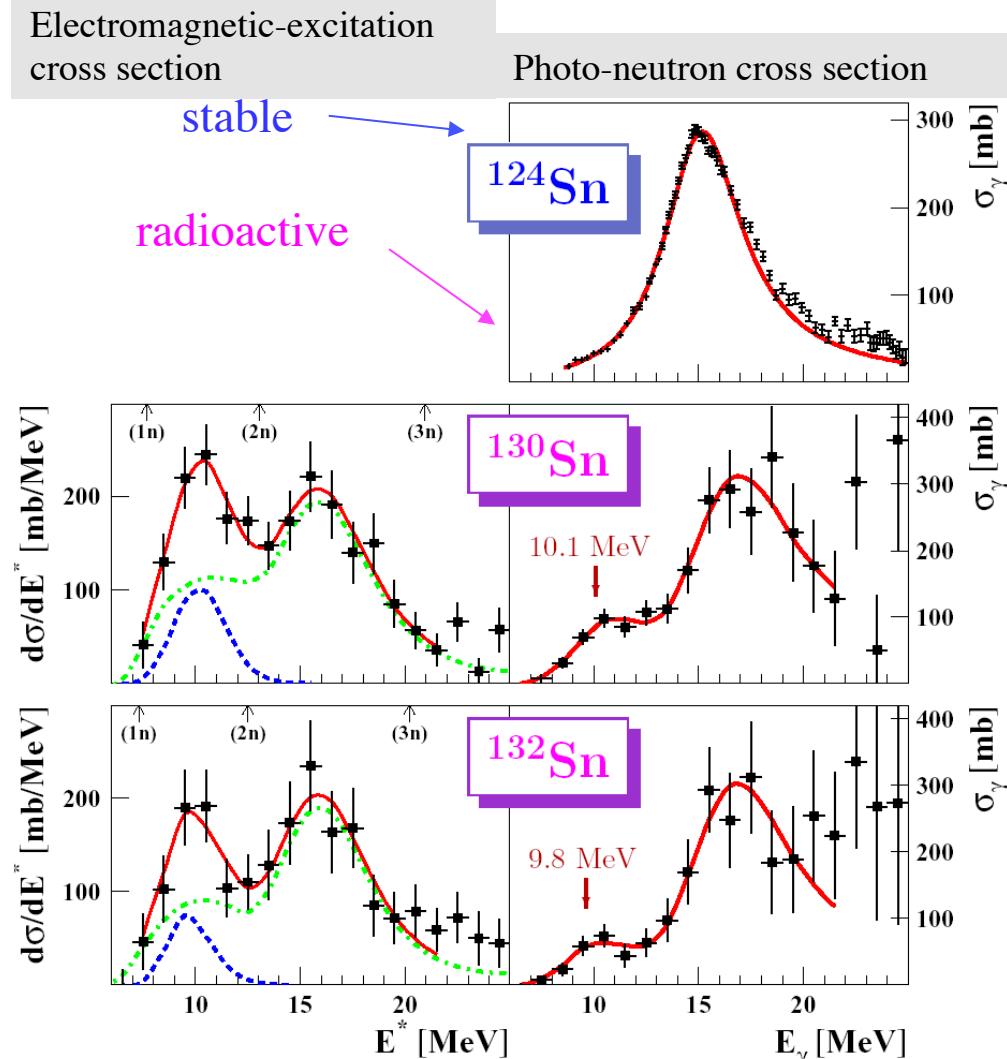
P. Adrich et al., PRL 95 (2005) 132501

(γ,γ') in ^{68}Ni using RISING

GDR
PDR
Total

$d\sigma/dE$ [mb/MeV]

E_γ [MeV]

Oliver Wieland et al.,
PRL 102, 092502 (2009)

PDR

- located at 10 MeV
- exhausts a few % TRK sum rule

GDR

- no deviation from systematics

Neutron kinetic energy
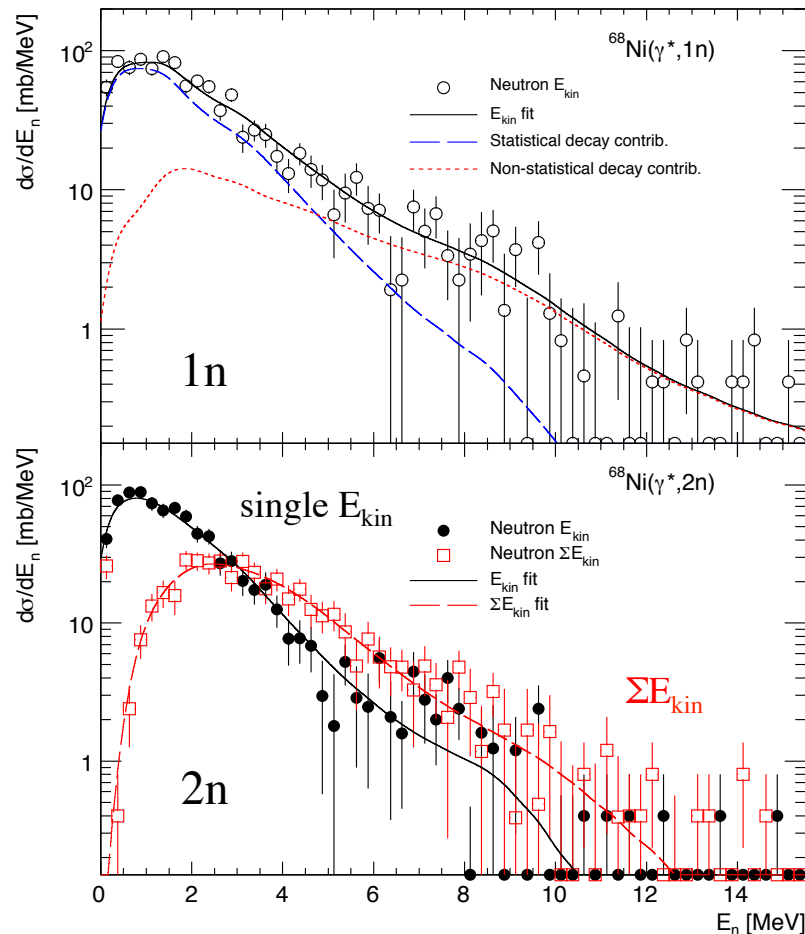
Gamma sum energy
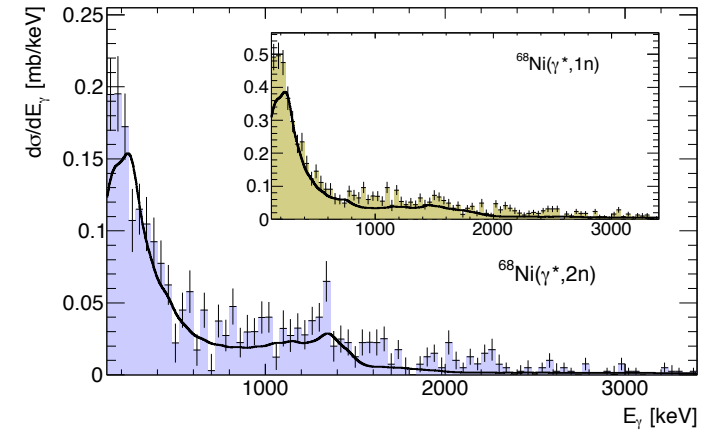
R_{direct} = 24(4) %

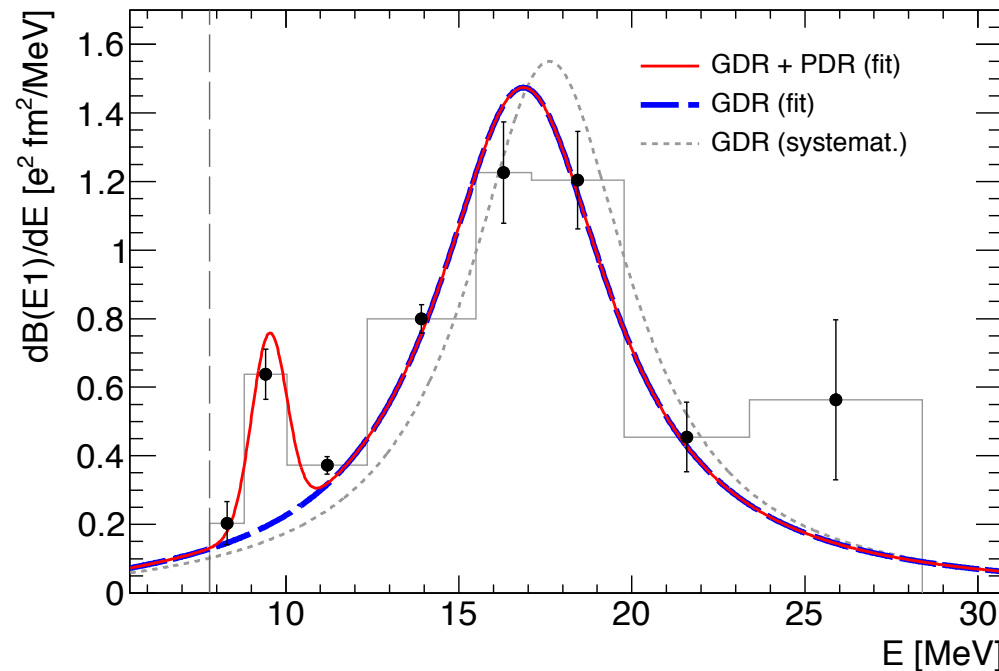## consistent fit taking into account:

1) invariant mass, but also information of subsets like $E_{kin}(n)$, E_{gsum} etc.

2) detailed knowledge about detector response function

D. Rossi et al., PRL 111 (2013) 242503

Simultaneous fit of spectra with 8 individual energy bins as free fit parameters: „deconvolution"

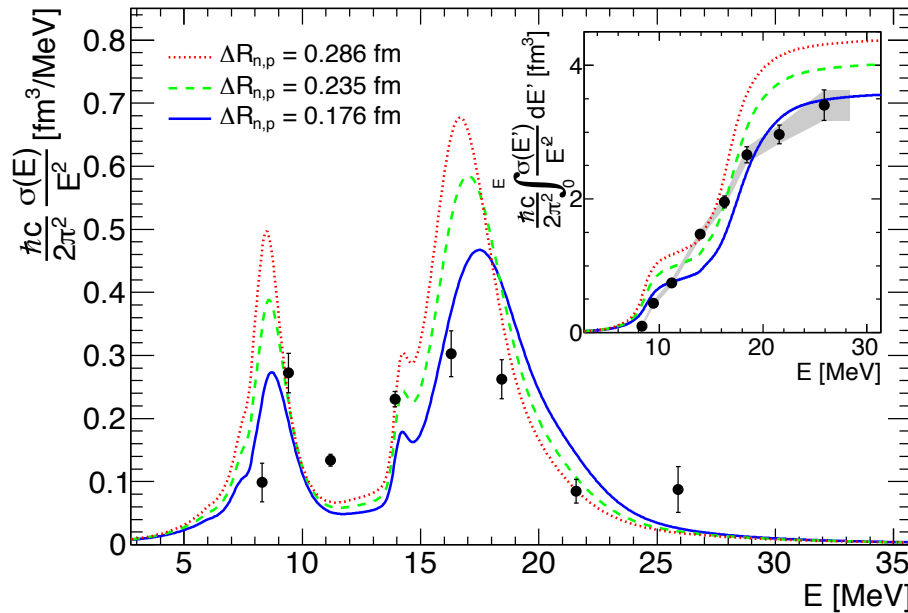|			This work	Lit.	Ref.
	E_m	[MeV]	17.1(2)	17.84	
GDR	Γ	[MeV]	6.1(5)	5.69	[30]
	S_{EWSR}	[%]	98(7)	100	
	E_m	[MeV]	9.55(17)	11	
PDR	σ	[MeV]	0.51(13)	< 1	[13, 25]
	S_{EWSR}	[%]	2.8(5)	5.0(1.5)	
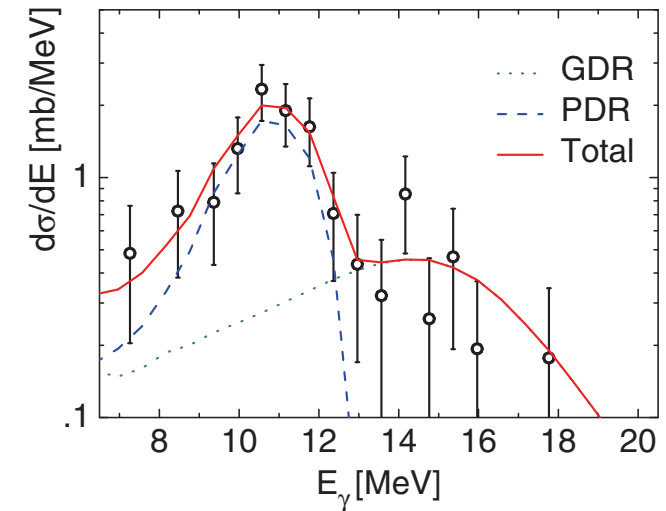
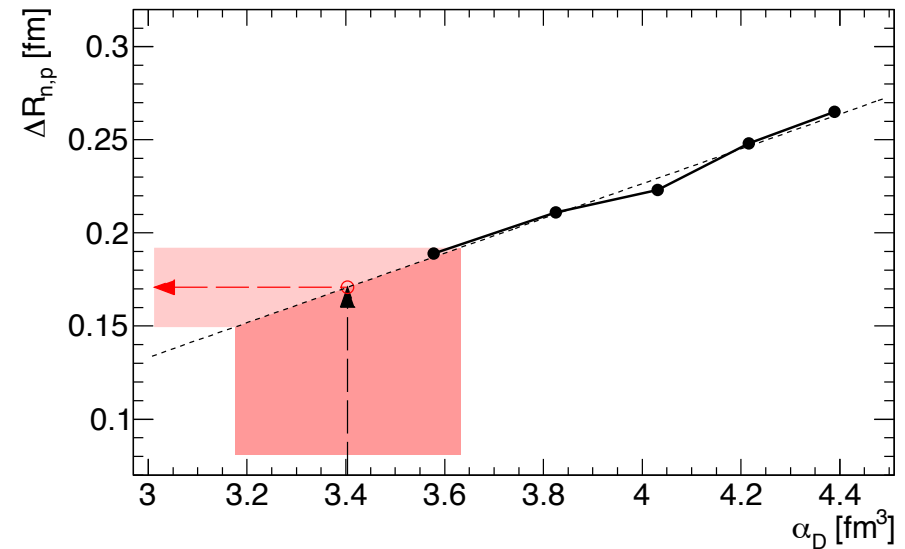O. Wieland et al., PRL 102, 092502 (2009)

Direct gamma-decay branching ratio
$\Gamma_0/\Gamma = 7(2)\%$

D. Rossi et al., PRL 111 (2013) 242503

$$\alpha_D = \frac{\hbar c}{2\pi^2} \int_0^\infty \frac{\sigma(E)}{E^2} dE$$

Theoretical calculations from
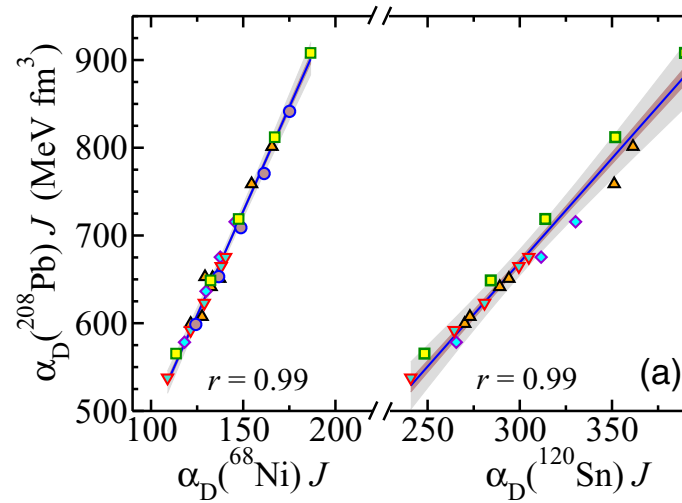J. Piekarewicz, PRC **83,** 034319 (2011)

Neutron-skin thickness
Using one particular RMF
interaction (Piekarewicz)

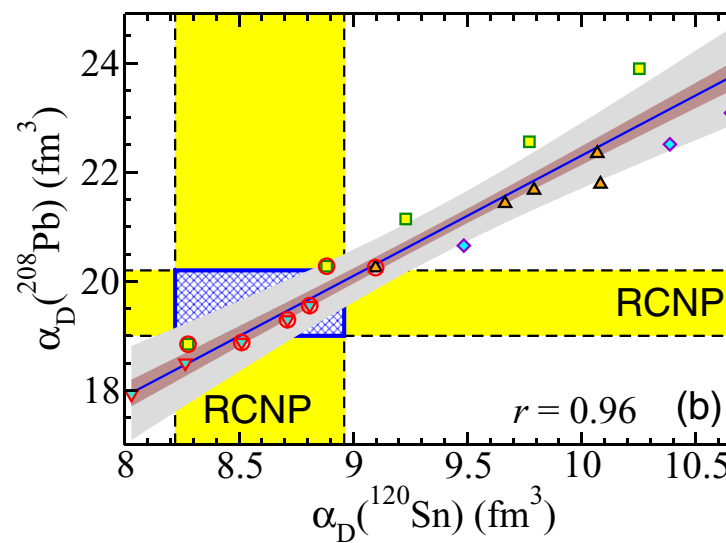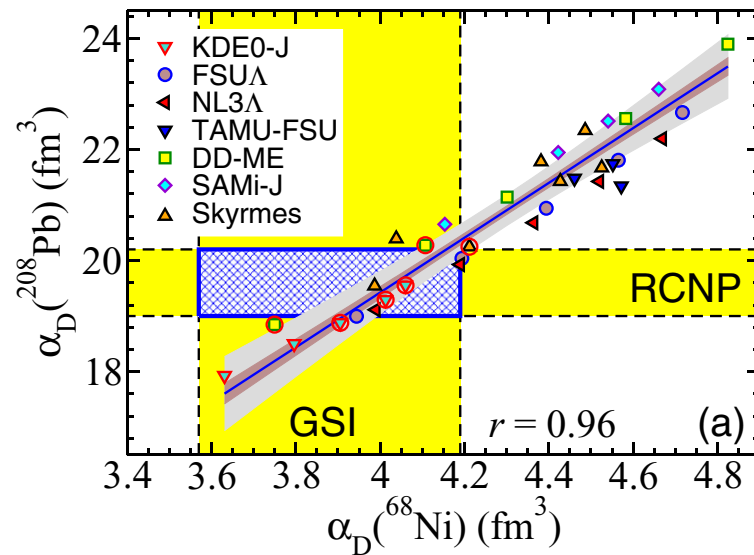$\Delta R_{n,p} = 0.175(21)$ fm

**Extracted value depends on
functional used !**

D. Rossi et al., PRL 111 (2013) 242503

Combined analysis of polarizabilities
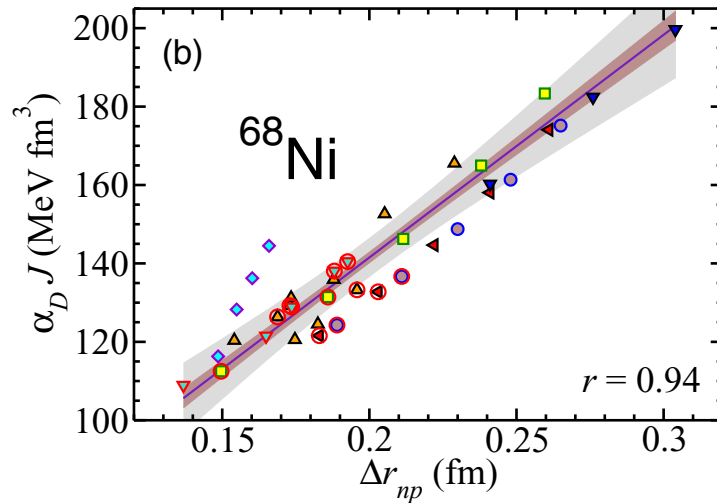
X. Roca-Maza et al., PRC 92 (2015) 064304

Data: ^{208}Pb: Tamii et al, PRL 107 (2011) 062502 | ^{68}Ni: D. Rossi et al., PRL 111 (2013) 242503 | ^{120}Sn: T. Hashimoto et al, PRC 92 (2015) 031305

Combined analysis of polarizabilities for ^{208}Pb, ^{120}Sn (RCNP), and ^{68}Ni (GSI)
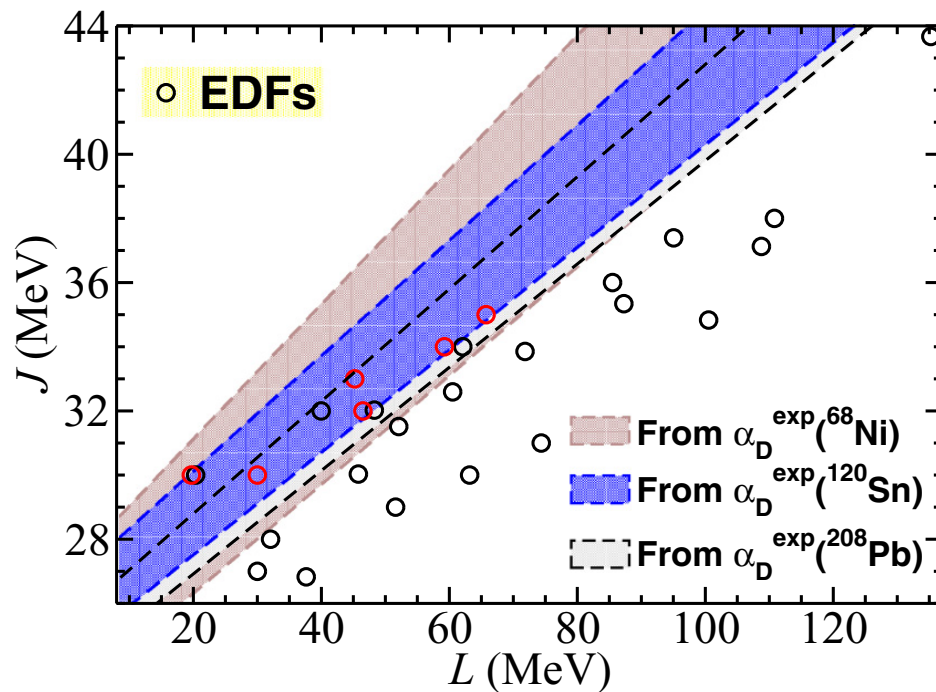
Xavi Roca-Maza et al.,
Phys. Rev. C 92 (2015) 064304

TABLE I. Various estimates of the neutron skin thickness (in fm) of ^{68}Ni, ^{120}Sn, and ^{208}Pb. (a) Lower and upper values of Δr_{np} as predicted by those models that reproduce the experimental values of the electric dipole polarizability of ^{68}Ni, ^{120}Sn, and ^{208}Pb. (b) Mean value and standard deviation of Δr_{np} as predicted by the same subset of models in column (a). (c) Predictions extracted from the correlation $\alpha_D J$-Δr_{np} using a suitable range for the symmetry energy coefficient J (see text for details).

Nucleus	Δr_{np} (a)	Δr_{np} (b)	Δr_{np} (c)
^{68}Ni	0.15–0.19	0.18 ± 0.01	0.16 ± 0.04
^{120}Sn	0.12–0.16	0.14 ± 0.02	0.12 ± 0.04
^{208}Pb	0.13–0.19	0.16 ± 0.02	0.16 ± 0.03

$$30 \leqslant J \leqslant 35 \, \text{MeV}$$

$$20 \leqslant L \leqslant 66 \, \text{MeV}$$

Measurement of the dipole polarizability of the unstable neutron-rich nucleus ^{68}Ni

D. M. Rossi,[1,2,*] P. Adrich,[1] F. Aksouh,[1,†] H. Alvarez-Pol,[3] T. Aumann,[4,1,‡] J. Benlliure,[3] M. Böhmer,[5] K. Boretzky,[1]
E. Casarejos,[6] M. Chartier,[7] A. Chatillon,[1] D. Cortina-Gil,[3] U. Datta Pramanik,[8] H. Emling,[1] O. Ershova,[9]
B. Fernandez-Dominguez,[3,7] H. Geissel,[1] M. Gorska,[1] M. Heil,[1] H. T. Johansson,[10,1] A. Junghans,[11] A. Kelic-Heil,[1]
O. Kiselev,[1,2] A. Klimkiewicz,[1,12] J. V. Kratz,[2] R. Krücken,[5] N. Kurz,[1] M. Labiche,[13,14] T. Le Bleis,[1,9,15] R. Lemmon,[14]
Yu. A. Litvinov,[1] K. Mahata,[1,16] P. Maierbeck,[5] A. Movsesyan,[4] T. Nilsson,[10] C. Nociforo,[1] R. Palit,[17] S. Paschalis,[4,7]
R. Plag,[9,1] R. Reifarth,[9,1] D. Savran,[18,19] H. Scheit,[4] H. Simon,[1] K. Sümmerer,[1] A. Wagner,[11] W. Waluś,[12]
H. Weick,[1] and M. Winkler[1]

[1]GSI Helmholtzzentrum für Schwerionenforschung GmbH, D-64291 Darmstadt, Germany
[2]Institut für Kernchemie, Johannes Gutenberg-Universität, D-55128 Mainz, Germany
[3]University of Santiago de Compostela, E-15705 Santiago de Compostela, Spain
[4]Institut für Kernphysik, Technische Universität Darmstadt, D-64289 Darmstadt, Germany
[5]Physik-Department E12, Technische Universität München, D-85748 Garching, Germany
[6]University of Vigo, E-36310 Vigo, Spain
[7]University of Liverpool, Liverpool L69 7ZE, United Kingdom
[8]Saha Institute of Nuclear Physics, Kolkata 700-064, India
[9]Institut für Angewandte Physik, Goethe Universität, D-60438 Frankfurt am Main, Germany
[10]Chalmers University of Technology, SE-41296 Göteborg, Sweden
[11]Helmholtz-Zentrum Dresden-Rossendorf e.V., D-01328 Dresden, Germany
[12]Jagiellonian University, PL-30-059 Krakow, Poland
[13]University of the West of Scotland, Paisley PA1 2BE, United Kingdom
[14]STFC Daresbury Laboratory, Warrington WA4 4AD, United Kingdom
[15]Institut Pluridisciplinaire Hubert Curien, F-67037 Strasbourg, France
[16]Bhabha Atomic Research Centre, Mumbai 400-085, India
[17]Tata Institute of Fundamental Research, Mumbai 400-005, India
[18]ExtreMe Matter Institute EMMI and Research Division, GSI Helmholtzzentrum für Schwerionenforschung GmbH,
D-64291 Darmstadt, Germany
[19]Frankfurt Institute for Advanced Studies, D-60438 Frankfurt am Main, Germany